



## 2 $\mu\text{m}$ soliton lasers in a bidirectional nonlinear polarization evolution $\text{Tm}^{3+}$ -doped fiber oscillator

Ni Feng<sup>a,b</sup>, Hui Hu<sup>a,b</sup>, Renlai Zhou<sup>a,b,\*</sup>, Encai Ji<sup>c,d</sup>, Xiaoxi Liu<sup>a,b</sup>, Hongcan Gu<sup>e,\*</sup>, K. Nakkeeran<sup>f</sup>

<sup>a</sup> Key Laboratory of In-Fiber Integrated Optics, Ministry Education of China, Harbin Engineering University, Harbin 150001, China

<sup>b</sup> College of Physics and Optoelectronic Engineering, Harbin Engineering University, Harbin 150001, China

<sup>c</sup> Shenzhen University, Shenzhen 518060, China

<sup>d</sup> MIL Medical Technology (Shenzhen) Co., Ltd, Shenzhen 518055, China

<sup>e</sup> Naval University of Engineering, Wuhan 430033, China

<sup>f</sup> School of Engineering, Fraser Noble Building, University of Aberdeen, Aberdeen AB243UE, UK

### ARTICLE INFO

#### Keywords:

2  $\mu\text{m}$  soliton lasers  
Nonlinear polarization evolution  
Mode-locked fiber laser

### ABSTRACT

We experimentally demonstrate a novel 2  $\mu\text{m}$  soliton laser using a bidirectional nonlinear polarization evolution mode-locked  $\text{Tm}^{3+}$ -doped fiber oscillator. The mode-locking operations between the laser signals propagating in clockwise and counterclockwise directions can be achieved through the intracavity polarization state adjustments independently, and the maximum achieved output powers are 332.5 and 367.8 mW with transfer efficiencies of 17.2 % and 18.3 %, respectively. Hysteresis in the output powers and spectra transformation between the two laser signals propagating in counter directions are observed and investigations are conducted in detail. Benefiting from the robust birefringence filtering effect, the central wavelength of this soliton laser can be continuously tuned from 1951.51 to 2015.89 nm. Stable high-order harmonic mode-locking (HML) operations are observed, and up to 633.02 MHz repetition rate with a central wavelength of 1992.55 nm is achieved. The monitored intensity spectra stability and average output power fluctuations exhibit excellent performance of this proposed 2  $\mu\text{m}$  soliton fiber laser. The phase noise levels in two counter directions propagating light signals are characterized at different average output powers. Our experiment provides a potential technique for the generation of 2  $\mu\text{m}$  solitons fiber laser that can be widely applied in ultrafast time-resolved measurements, mid-infrared frequency metrology, molecular spectroscopy, etc.

### Introduction

Ultrafast soliton fiber lasers operating around 2  $\mu\text{m}$  wavelength region have attracted great interest because of their intrinsic advantages of eye safety, low-loss atmospheric transmission window and water-absorbing band, which can be effectively utilized in laser surgery [1], transparent material micro-machining [2], and free space optical communications [3]. Specially, 2  $\mu\text{m}$  ultrashort pulse lasers are suitable for effective accession of the mid/far-infrared spectral regions via nonlinear frequency conversion [4]. The mid/far-infrared spectral regions cover the primary vibrational absorption bands of most chemical and biological molecules as well as the “fingerprint region” [5], which are essential for thermal imaging, infrared homing, and countermeasures. To generate 2  $\mu\text{m}$  ultrashort pulses in fiber lasers, quite commonly, thulium

( $\text{Tm}^{3+}$ )-doped, Holmium ( $\text{Ho}^{3+}$ )-doped, and  $\text{Tm}^{3+}/\text{Ho}^{3+}$  co-doped fibers are optionally deployed as the gain fibers in the cavity [6]. Among them,  $\text{Tm}^{3+}$ -doped fiber (TDF) exhibits some distinctive advantages. Firstly, it possesses a 1700–2100 nm wide gain bandwidth that supports the direct generation and/or amplification of less than 100 fs ultrashort pulses in the cavity, and the central wavelength of the soliton pulses can be flexibly tuned and selected in a wide spectral range [7]. More interestingly, multiwavelength mode-locking operations, including dual-/trip-wavelength [8] and four-wavelength [9], can be achieved in TDF lasers, when the gain competitions among the multiple oscillation wavelengths are balanced by the appropriate spectral filtering of the intracavity light signal. Additionally,  $\text{Tm}^{3+}$  ion is asserted as one of the most efficient laser-active ions, and the TDF can be in-band pumped by high powered  $\text{Er}^{3+}$ -doped fiber (EDF) laser with high conversion

\* Corresponding authors.

E-mail addresses: [zhourl@hrbeu.edu.cn](mailto:zhourl@hrbeu.edu.cn) (R. Zhou), [tankomb@163.com](mailto:tankomb@163.com) (H. Gu).

<https://doi.org/10.1016/j.rinp.2022.105930>

Received 5 July 2022; Received in revised form 9 August 2022; Accepted 19 August 2022

Available online 23 August 2022

2211-3797/© 2022 Published by Elsevier B.V. This is an open access article under the CC BY-NC-ND license (<http://creativecommons.org/licenses/by-nc-nd/4.0/>).

efficiency and lower thermal load [6].

Hitherto, the conventional [7], dissipative [10], dispersion-managed [11] and self-similar solitons [12] have been generated in TDF lasers via various mode-locking techniques, mainly including 2D saturable absorbers (SAs) [7,10,11], nonlinear fiber loop mirrors (NOLM) [7,12], and nonlinear polarization evolution (NPE) [13]. Main drawback in utilizing the 2D SAs is the switching performance tends to degrade over time, which may impede long-term mode-locking stability and its application regime. In case of the NOLM, the ability to self-start the mode-locking operation is always weak, and hence auxiliary vibration and percussion are employed to assist the buildup of mode-locking. NPE mode-locked technique has been demonstrated to be a powerful approach to overcome the aforementioned drawbacks in 2D SAs and NOLM, which also possesses some inherent advantages like the high damage threshold, large modulation depth, and rapid saturation absorption [14,15]. As an emerging ultrafast light source design technology, a bidirectional NPE mode-locked fiber oscillator demonstrated to generate high-energy dual-comb laser signals from counterpropagating directions in a single cavity [16]. Due to the intrinsic cavity asymmetry, the mode-locked spectra and power evolutions between the two counterpropagating signals exhibited different characteristics. Until now, 2  $\mu\text{m}$  wavelength regime soliton lasers have never been reported or investigated in the bidirectional NPE fiber oscillators. Owing to the versatility of the NPE mode-locked techniques achievable through manipulation of the cavity parameters like, pumping rate, intracavity polarization state, and cavity length, the mode-locking operation between the laser signals propagating in the clockwise (CW) and counter-clockwise (CCW) directions can be achieved independently. Nonlinear dynamics attached to this switching process need to be investigated in detail, for the understanding of the working principle and as well the controlling of 2  $\mu\text{m}$  soliton laser in bidirectional NPE mode-locked fiber laser.

In this work as a novel attempt, we experimentally investigate the possibility of generating 2  $\mu\text{m}$  soliton pulses in a bidirectional NPE mode-locked TDF oscillator. In the proposed fiber laser, mode-locking operation can be desirably switched to lase either in the CW or CCW direction through a fine manipulation of the intracavity polarization state. Hysteresis observed in the output powers and spectra transformation in the counter directions propagating signals are studied in detail. Due to the robust birefringence filtering effect, wideband wavelength tuning of the mode-locked TDF laser is achieved through appropriate adjustments of the waveplates position. Stable high-order harmonic mode-locking operation is realized, and the measurements corresponding to the oscilloscope trace, radio frequency spectrum and output spectra are reported. To evaluate the stable performance of the proposed 2  $\mu\text{m}$  soliton fiber laser, monitoring of the intensity spectra, average output power fluctuations and phase noise level are carried out. Starting with the experimental setup, followed by the operating procedure, we report all the results in this research investigation on the proposed highly stable multifunctional soliton fiber laser which can be constructed and controlled for laser signal output around 2  $\mu\text{m}$  wavelength regime for various applications.

## Experiment setup

Experimental setup of the proposed mode-locked TDF laser is shown in Fig. 1(a). In contrast to traditional NPE mode-locked fiber lasers, the polarization-insensitive isolator is removed to realize the bidirectional lasing in the cavity. A 30 cm-long highly TDF (Nufern) is used as the gain medium. A two-stage 1565.5 nm fiber amplifier is selected as pump source and coupled into TDF through a 1560/2000 nm wavelength-division multiplexer (WDM), and the maximum output power is 10 W. Spliced loss between WDM and fiber amplifier is  $\sim 5\%$ , and the maximum coupled power is  $\sim 3$  W. Two matching fiber collimators are employed to reshaped the intracavity light beam, and the coupling efficiency between two fiber collimators is  $\sim 81\%$  through two assemblies of a precise optical adjustment bracket and a rotary platform. Two half-

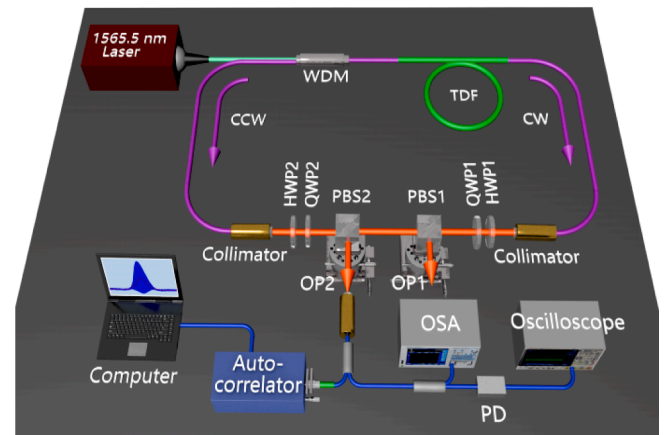


Fig. 1. Schematic diagram of bidirectional mode-locked TDF laser.

wave plates (HWPs) and two quarter-wave plates (QWPs) are included to adjust and select the polarization states of the bidirectional optical signals in the cavity. Two polarization beam splitters (PBSs) are used to export the solitons lasing in both directions. The laser spectrum and output pulse train are measured by an optical spectrum analyzer (AQ6375B, Yokogawa) with a resolution of 0.02 nm and a real-time oscilloscope (MSO64, Tektronix) with a high-speed InGaAs photodiode detector (818-BB-51). A radio frequency (RF) signal analyzer (Rohde & Schwarz) with a 10 Hz–40 GHz bandwidth is utilized to monitor the soliton pulses frequency. The fine structure of mode-locked pulses is analyzed by a commercial autocorrelator (SM-2000, APE). The average output power is measured by a power meter (S470C, Thorlabs) with 100  $\mu\text{W}$ –5 W power range and 250 nm–10.6  $\mu\text{m}$  wavelength range.

## Experiment results and discussion

Mode-locking operations in two counter directions can be independently achieved at a certain pump power by adjusting the waveplates orientation to get suitable cavity loss. Self-starting threshold of mode-locking in CW direction is  $\sim 750$  mW. Measured output spectra of the mode-locked pulses are shown in Fig. 2(a), the blue curve is logarithmic scale (Log), and the red curve is linear scale (Lin). Measured 3-dB spectral bandwidth is 6.9 nm with a central wavelength of 1979.71 nm. High-order symmetrical Kelly-sidebands are observed in the spectra, indicating that there is strong resonant coupling between the soliton and dispersive wave, which results from the periodic perturbations caused by the discrete nature of the loss, dispersion, and nonlinearity devices in this proposed cavity [17]. In addition, two dip sidebands are also observed in the spectra. These characteristics can be attributed to the four-wave-mixing process between the soliton and dispersive waves induced by the periodic soliton parameter variation [18]. Based on the formation mechanism, the Kelly sidebands always share intracavity energy with soliton, and the pure solitons can be separated from the resonant continuous wave background by utilizing nonlinear Fourier transform (NFT) [19,20]. The fine structure of soliton pulses is exhibited in Fig. 2(b). The full width half maximum (FWHM) of pulse duration is 1.12 ps calculated through a hyperbolic secant squared ( $\text{sech}^2$ ) profile fit. Time-bandwidth product (TBP) was calculated as  $\sim 0.591$ , indicating that the output pulses were slightly chirped and widened. The oscilloscope trace of the pulse train is depicted in Fig. 2(c). The pulses period is about 18.95 ns, which is consistent with the roundtrip time of the laser cavity. Screenshot of the pulses train with 10  $\mu\text{s}$  time range is shown in the inset of Fig. 2(c). Entire temporal pulse profile is constant and stable without any fluctuations.

By appropriately adjusting the HWP1 and QWP1 in the cavity, the mode-locking in CCW direction can be established, and the self-starting threshold is  $\sim 700$  mW, which is lower than that in CW direction



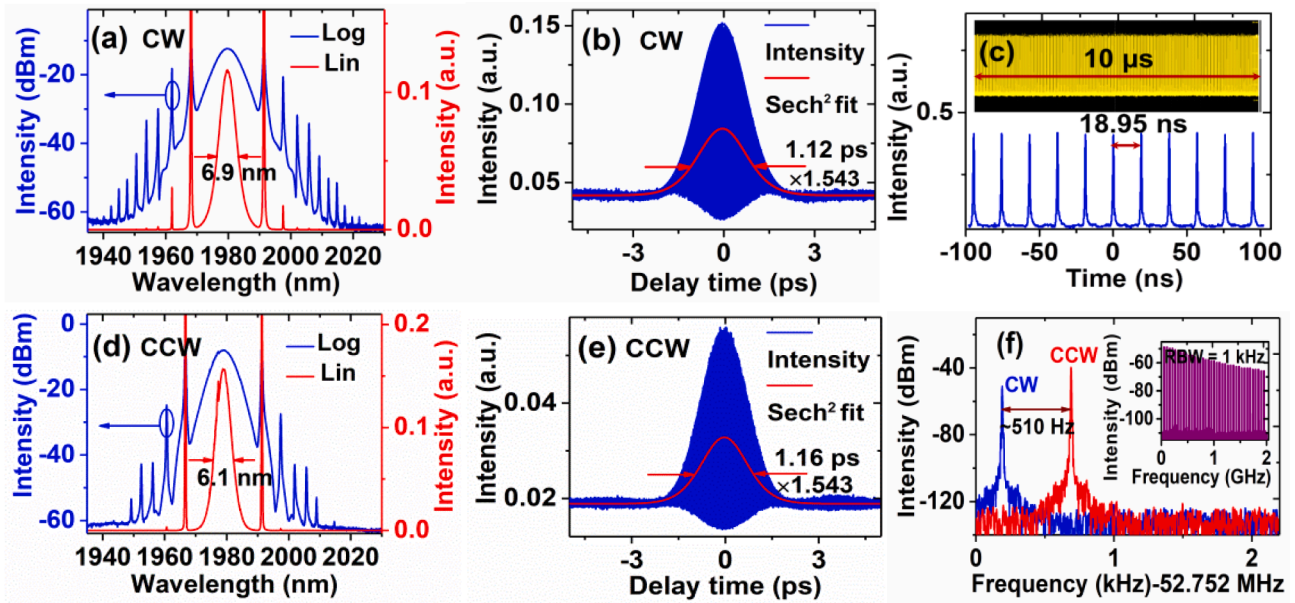


Fig. 2. Experiment results of mode-locked TDF laser: (a), (d) output spectra in CW and CCW directions; (b), (e) corresponding intensity autocorrelation traces; (c) output pulses trains; (f) RF spectra of soliton pulses.

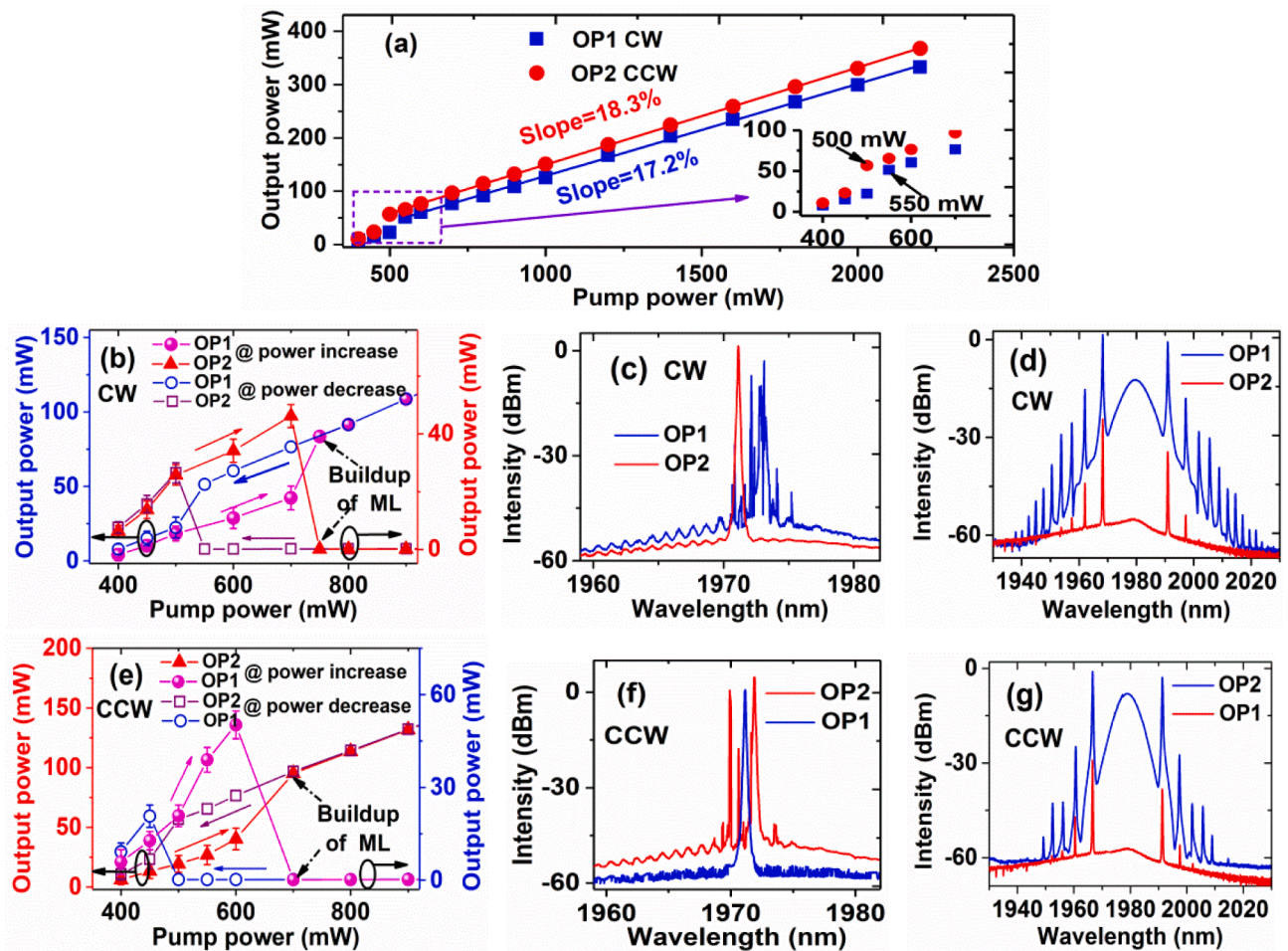


Fig. 3. Output characteristics of the 2  $\mu\text{m}$  mode-locking operation in CW and CCW directions: (a) average output power versus the 1565.5 nm pump power; (b), (e) hysteresis of output powers in OP1 and OP2; (c), (d) output spectra transformation in OP1 and OP2 for the mode-locking in CW direction; (f), (g) output spectra transformation in OP1 and OP2 for the mode-locking in CCW direction.

counterpart. The 3-dB spectral bandwidth is 6.1 nm with a central wavelength of 1979.26 nm as shown in Fig. 2(d). A continuous-wave laser signal at a wavelength of 1977.28 nm is also found in the spectrum. Measured intensity autocorrelation trace is presented in Fig. 2(e), and the FWHM pulse duration of 1.16 ps is calculated using a  $\text{sech}^2$  profile fit, and the calculated TBP is  $\sim 0.541$ . The RF spectrum distributions of soliton pulses in both directions (CW and CCW) are presented in Fig. 2(f) with a resolution bandwidth (RBW) of 10 Hz and a span of 2.2 kHz. The pulses repetition rate is  $\sim 52.752$  MHz, which is in accordance with the fundamental repetition rate of the lasing cavity. Due to the different group delays of two counter directional soliton pulses, a repetition rate difference of  $\sim 510$  Hz is displayed in Fig. 2(f). The signal-to-noise ratios (SNRs) of the bidirectional soliton pulses are  $\sim 55.2$  dB (CW) and  $\sim 67.5$  dB (CCW), confirming stable mode-locked operations. Up to 2 GHz wideband RF spectrum with 1 kHz RBW is depicted in the inset of Fig. 2(f), and no envelope modulation is found.

The variations in the average output power with respect to different pump powers are measured as shown in Fig. 3(a). The average output powers of soliton pulses in CW and CCW directions increase linearly along with the pump power with respective slope efficiency of 17.2 % and 18.3 %. At a pump power of 2200 mW, the maximum output powers of 332.5 and 367.7 mW are achieved without reaching saturation. Owing to the pumping hysteresis effect, the mode-locking operations can be maintained at 550 mW (CW) and 500 mW (CCW) which are far lower the self-started mode-locked thresholds, as shown in the inset of Fig. 3 (a). For further studying of the hysteresis effect in the bidirectional mode-locked laser signals, we monitor the variations of output powers at OP1 (CW) and OP2 (CCW) as depicted in Fig. 3(b) and (e). Before mode-locking formation, both output powers at OP1, OP2 exhibit dramatic fluctuations due to the strong gain competition between the CW and CCW directions laser signals. When the pump power is increased to the self-starting threshold (750 mW for CW and 700 mW for CCW), abrupt jumps, both upward and downward, at the output powers are observed. For the mode-locked laser signal, the output power sharply jumps upward from 42.3 to 83.5 mW in CW direction and from 40.3 to 95.2 mW in CCW direction, implying the buildup of mode-locking in the cavity. Meanwhile, the output powers of the counter propagating laser signals sharply jump downward from 42.6 to 0.13 mW in CCW direction and from 50.2 to 0.12 mW in CW direction. When the pump power is decreased below the unlocking threshold (550 mW for CW and 500 mW for CCW), reverse hysteresis process can also be observed. It can be noted that the output powers abruptly jump downward from 51.5 to 22.4 mW for CW in Fig. 3(b), and from 56.8 to 23.2 mW for CCW in Fig. 3(e), while the output powers of laser signals in counter direction abruptly jumps upward from 0.13 to 26.6 mW and from 0.17 to 20.7 mW.

As shown in Fig. 3(c) and (f), the output spectra are the free-oscillating continuous-wave lasers before the mode-locking formation, where the intensity fluctuations in the spectra imply the drastic turbulence of output powers of laser signals in both oscillation directions. When the mode-locking is established in either one of the directions, the unlocked laser signal in the counter direction is strongly suppressed. Measured output spectra are shown in Fig. 3(d) and (g). Typical mode-locked spectra are observed in the mode-locked direction, while only some weak wavelength peaks can be seen in the counter direction. It should be noticed that the weak wavelength peaks are consistent with the Kelly sidebands of the mode-locked spectra in CW and CCW directions. To identify whether they belong to the mode-locking operation, the weak laser signals are magnified by a TDF amplifier, then coupled into a high-speed photodiode detector. However, no pulses trains are observed by the oscilloscope, hence we consider the wavelength peaks belong to the weak continuous-wave laser in the cavity. For the NPR mode-locking in our experiment, the saturable absorption depends on accumulated nonlinear phase shifts along the two counter directions in fiber cavity and the appropriate intracavity polarization loss [21]. Through appropriately adjusting the HWP1, QWP1, HWP2, and

QWP2 control, the unidirectional mode-locking operation in CCW or CW direction can be achieved independently, but the bidirectional mode-locking operation in Ref. [16] cannot be obtained, regardless of an increase in pump power, double-way pumping and finely adjusting waveplates in the cavity.

The long-term stability of the proposed mode-locked TDF laser is assessed in a lab environment at room temperature. The intensity spectra are repeatedly recorded at every 5-minutes interval for 150 min using the OSA, and reconstructed intensity spectral evolution is displayed in Fig. 4(a). High spectral reliability in terms of the central wavelengths, Kelly sidebands and 3 dB-bandwidths are exhibited, which indicates the stable operation of the mode-locked state in the cavity. Fluctuations of the average output power for the pump power kept constant at 1000 mW are monitored for 150 min. As presented in Fig. 4 (b), the calculated root mean square (RMS) and peak-peak of the output power fluctuations are  $\sim 0.38$  % and  $\sim 1.45$  %, respectively, which again demonstrate excellent long-term stability of the bidirectional 2  $\mu\text{m}$  wavelength mode-locked fiber laser.

Owing to the robust birefringence filtering effect in the cavity, broadband tunable mode-locked TDF laser is achieved in the experiment. Keeping the pump power fixed at 800 mW, the central wavelength can be tuned from 1951.51 to 2015.89 nm through elaborate adjustments of the HWPs and QWPs. Fig. 5(a) shows the output spectra tuning of the central wavelength in steps of  $\sim 7$  nm, and this tuning process is exactly retractable. As the mode-locked laser is tuned towards the longer wavelength side, more and more sideband peaks occur in the spectra, and comparatively converge on the blue-side of the central wavelength. Especially in P9 and P10 states, a series of wavelength peaks occur in the spectra, as seen dotted box in Fig. 5(a), which affects the stability of the mode-locking operation in the cavity. Similar to the Kelly sidebands, these resonant sidebands result from the coupling between continuous-wave and dispersive waves [22]. Variations of the output power and 3-

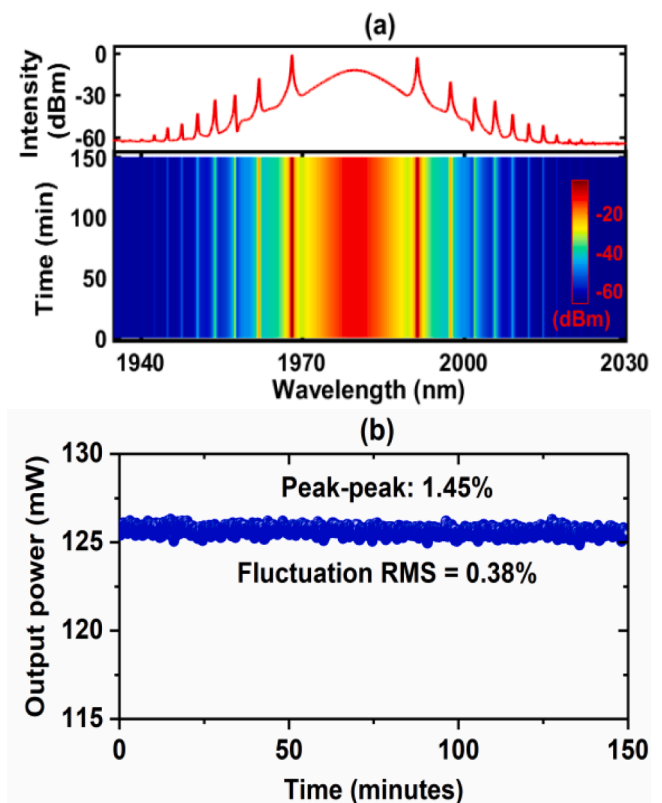


Fig. 4. (a) Intensity spectral evolution repeatedly recorded with 5-minute interval for 150 min; (b) average output power fluctuations at a pump power of 1000 mW.



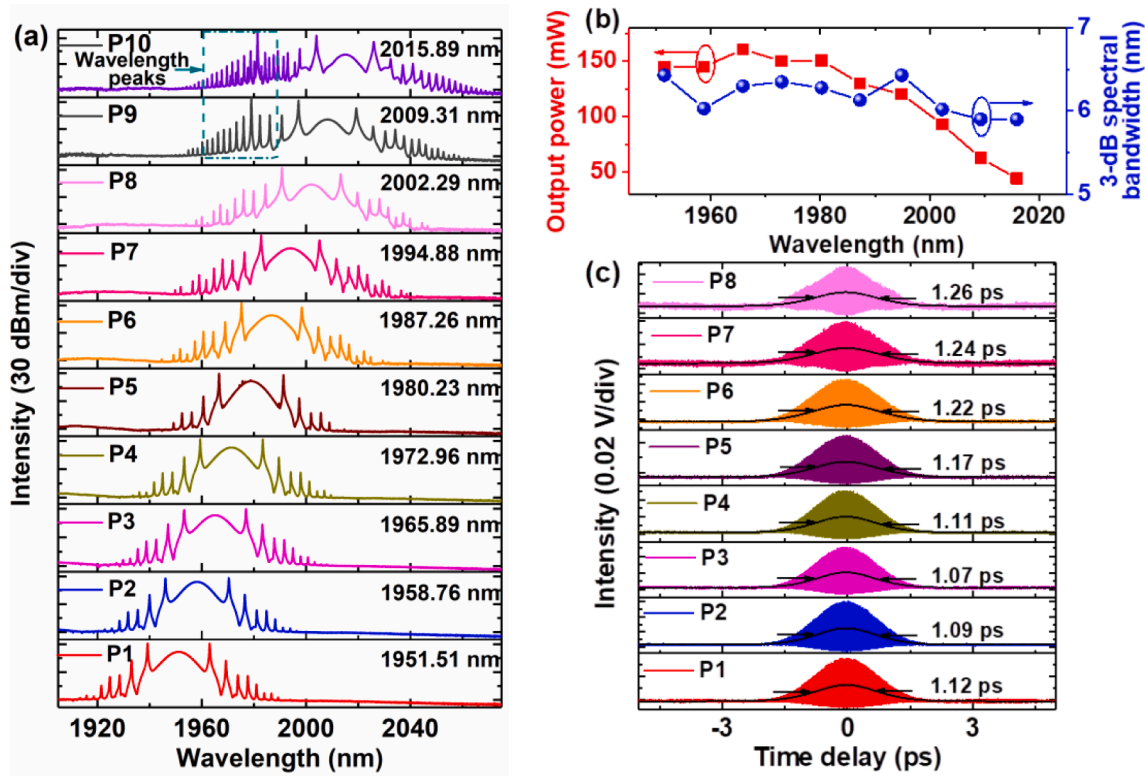


Fig. 5. Wavelength tuning process of mode-locked TDF laser: (a) output spectra ranging from 1951.51 nm to 2015.89 nm; (b) variations of output power and 3-dB spectral bandwidth; (c) intensity autocorrelation traces of P1-P8 state.

dB spectral bandwidth are depicted in Fig. 5(b). It is observed that the output power initially grows from 144.80 mW (P1) to and 160.62 mW (P3), and then gradually descends to 44.25 mW (P10). 3-dB spectral bandwidth varies from 5.90 nm to 6.43 nm. The measured pulse widths of P1-P8 states are displayed in Fig. 5(c). Wavelength tuning of P1 (1.12 ps at 1951.51 nm) to P2 (1.09 ps at 1958.76 nm) to P3 (1.07 ps at 1965.89 nm) states generates chirped soliton pulses of pulse width getting compressed feature. And for further tuning towards the longer

wavelength, the chirped pulse width varies from 1.07 to 1.26 ps. The pulse widths variation feature for P1-P10 states is opposite to that of the output powers characteristics shown in Fig. 5(b). The shortest chirped pulse duration is obtained in P3 (1.07 ps at 1965.89 nm) state. No stable mode-locked operation observed for P9 or P10 states, and hence no results report for their pulse width measurements.

For conventional solitons operation in anomalous dispersion regime, energy quantization effect leads to the single pulse in the cavity splitting

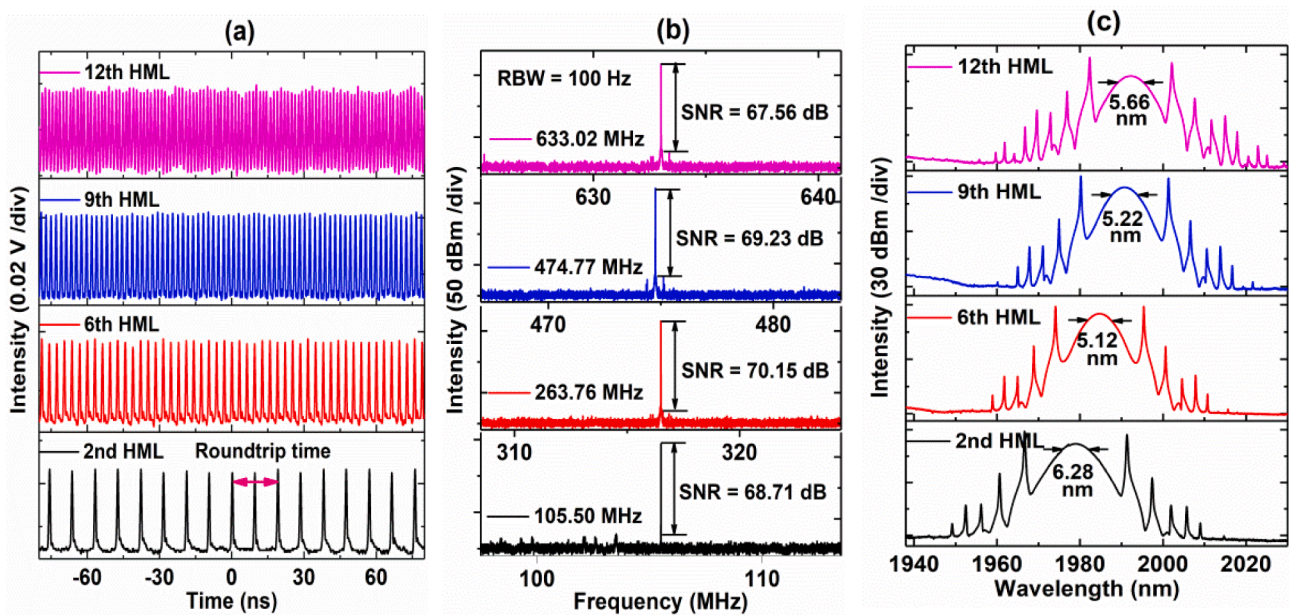


Fig. 6. (a) Out pulse trains of 2nd-, 6th-, 9th- and 12th-order HML operations; (b) RF spectra at repetition rate of 105.50, 263.76, 474.77 and 633.02 MHz; (c) output spectra of 2nd-, 6th-, 9th- and 12th-order HML solitons.

into random multi-pulses [23]. Through the soliton-dispersive wave interactions [24] and complex soliton-soliton attraction / repulsion force [25], the multi-pulses can self-arrange to generate a stable and equidistant spaced pulse train with repetition rates far beyond the fundamental repetition rate, namely harmonic mode-locked (HML) operation. In our proposed mode-locked TDF laser, stable high-order HML operations are achieved by elaborately rotating the waveplates at a pump power of 1000 mW. Pulse repetition rate can be tuned from 52.75 to 633.02 MHz, corresponding to the fundamental mode-locking frequency up to 12th-order HML. The output pulse trains of 2nd-, 6th-, 9th- and 12th-order HML operations are recorded as shown in Fig. 6(a), and their pulse repetition rates are 105.50, 263.76, 474.77 and 633.02 MHz, respectively. Fig. 6(b) displays the measured RF spectra of aforementioned HML pulses in 16-MHz span with RBW of 100 Hz, respectively. As can be shown from Fig. 6(b) that the SNRs of all RF signals are better than 67 dB, indicating the HML operate in a stable regime. Fig. 6(b) depicts the SNRs of all RF signals are better than 67 dB, indicating that the HML are all operating in a stable regime. The corresponding output spectra are displayed in Fig. 6(c). The central wavelengths are 1979.31, 1984.81, 1990.88, and 1992.55 nm, and their 3-dB spectral bandwidths are 6.28, 5.12, 5.22 and 5.66 nm.

Noise characteristic is an important specification of any mode-locked fiber laser, which might need to meet the requirements of a good-quality seed coherent light source for other sophisticated ultrafast laser systems. To investigate the noise characteristic of the proposed bidirectional 2  $\mu\text{m}$  wavelength mode-locked fiber laser, we measured the phase noise spectra corresponding to various output powers. The mode-locked pulses are coupled to a high-speed InGaAs photodiode detector, and the generated electrical signals are characterized by a phase noise analyzer (Rohde & Schwarz). Fig. 7(a), (b) depict the phase noise spectra of the mode-locked pulses in CW and CCW directions for the offset frequencies range from 10 Hz to 10 MHz. For the mode-locking in CW direction, the phase noise levels corresponding to output powers of 51.4 mW and 124.9 mW show a similar downward tendency. In the offset frequencies ranging from 10 Hz to 1.4 kHz, the phase noise level abruptly drops from  $-23.4$  dBc/Hz to  $-106.2$  dBc/Hz, and then gradually descend to the

lowest value of 127.2 dBc/Hz. For the mode-locked operation in the CCW direction, similar performance observed as reported in Fig. 7(b). Compared with these phase noise spectra with that of the NPE mode-locked ytterbium-doped fiber laser [26], the phase noise level of the bidirectional 2  $\mu\text{m}$  wavelength mode-locked fiber laser is higher, and this might be due the following reasons. Firstly, the phase noise is sensitive to the net cavity dispersion, and a lower cavity dispersion is beneficial for generation of solitons pulses with lower phase noise level [26]. Due to the typically high amount of anomalous group velocity dispersion of silica-fiber operated under 2  $\mu\text{m}$  region, the mode-locked TDF laser operates in strong negative dispersion regime and hence the phase noise level of solitons pulses is highly increased. Secondly, the poor shelter in our case also results in a higher phase noise level, such as the thermal management of gain fiber, additional noise from the 1565.5 nm fiber amplifier and environmental perturbations. We believe the noise characteristic of our proposed mode-locked TDF laser can be improved through optimization of the above-mentioned parameters.

## Conclusion

To conclude, we experimentally demonstrate a novel 2  $\mu\text{m}$  soliton fiber laser employing a bidirectional NPE mode-locked TDF oscillator. By suitable positions for the QWPs and HWP in the cavity, the 2  $\mu\text{m}$  mode-locking operations can be selected between the CW and CCW directions and the maximum achieved output powers are 332.5 (CW) and 367.8 mW (CCW) with a transfer efficiency of 17.2 % and 18.3 %, respectively. The hysteresis effect of output powers and spectral transformation are observed for the mode-locking operations in both the CW and CCW directions. Benefiting from the robust birefringence filtering effect, the central wavelength of soliton laser can also be continuously tuned from 1951.51 nm to 2015.89 nm. Stable high-order HML operations are achieved, and up to 633.02 MHz (12th-order HML) repetition rate with a central wavelength of 1992.55 nm is obtained. The intensity spectra stability and average output power fluctuations are monitored in the course of sustained 150 min operations, that exhibited excellent long-term stable and reliable output(s) of the proposed 2  $\mu\text{m}$  soliton fiber laser. The phase noise levels of the 2  $\mu\text{m}$  soliton fiber laser are characterized in both directions operation independently, which can be improved through optimization of the laser system and environmental parameters. Our experiment provides a potential technique for the generation of 2  $\mu\text{m}$  solitons fiber laser that can be utilized for many applications that include molecular spectroscopy, ultrafast time-resolved measurement, etc.

## Funding

This work is financially supported by National Natural Science Foundation of China (61905150; 61805281); Fundamental Research Funds for the Central Universities, China (Grant No. 3072022CFJ2501; 3072022CF2506); Natural Science Foundation of Guangdong Province, China (2019A1515010732).

## CRediT authorship contribution statement

Ni Feng: . Hui Hu: . Renlai Zhou: Methodology, Writing – original draft. Encai Ji: Supervision. Xiaoxi Liu: Software. Hongcan Gu: Methodology, Writing – review & editing. K. Nakkeeran: Conceptualization, Resources, Writing – review & editing.

## Declaration of Competing Interest

The authors declare that they have no known competing financial interests or personal relationships that could have appeared to influence the work reported in this paper.

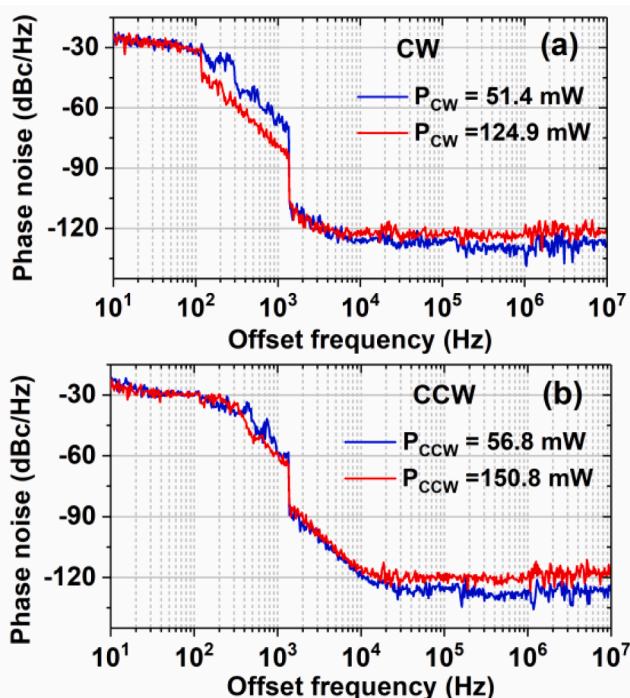


Fig. 7. Measured phase noise levels of 2  $\mu\text{m}$  soliton pulses at different output powers: (a) 51.4 and 124.9 mW in CW direction, (b) 56.8 and 150.8 mW in CCW direction.

## Data availability

Data will be made available on request.

## References

- [1] Hüttmann, Yao C, Endl E. New concepts in laser medicine: Towards a laser surgery with cellular precision. *Lasers Med Sci* 2015;20:135–9.
- [2] Gattass RR, Mazur E. Femtosecond laser micromachining in transparent materials. *Nat Photon* 2008;2:219–25.
- [3] Soref R. Enabling 2  $\mu\text{m}$  communications. *Nat Photon* 2015;9(6):358–9.
- [4] Zhang J, Mak KF, Nagl N, Seidel M, Bauer D, Sutter D, et al. Multi-mW, few-cycle mid-infrared continuum spanning from 500 to 2250  $\text{cm}^{-1}$ . *Light Sci Appl* 2018;7:17180.
- [5] Schliesser A, Picqué N, Hänsch TW. Mid-infrared frequency combs. *Nat Photon* 2012;6:440–9.
- [6] Kirsch DC, Chen S, Sidharthan R, Chen Y, Yoo S, Chernysheva M. Short-wave IR ultrafast fiber laser systems: current challenges and prospective applications. *J Appl Phys* 2020;128:180906.
- [7] Dai R, Meng Y, Li Y, Qin J, Zhu S, Wang F. Nanotube mode-locked, wavelength and pulsewidth tunable thulium fiber laser. *Opt Express* 2019;27:3518–27.
- [8] Li H, Hu F, Li C, Tian Y, Huang C, Zhang J, et al. Generation of switchable multiwavelength solitons with wide wavelength spacing at 2  $\mu\text{m}$ . *Opt Lett* 2019;44:2442–5.
- [9] Yan Z, Sun B, Li X, Luo J, Shum PP, Yu X, et al. Widely tunable Tm-doped mode-locked all-fiber laser. *Sci Rep* 2015;6:27245.
- [10] Watanabe K, Zhou Y, Sakakibara Y, Saito T, Nishizawa N. Dispersion-managed, high-power, Tm-doped ultrashort pulse fiber laser using single-wall-carbon-nanotube polyimide film. *OSA Continuum* 2021;4:137–48.
- [11] Michalska M. Dispersion managed thulium-doped fiber laser mode-locked by the nonlinear loop mirror. *Opt Laser Technol* 2021;138:106923.
- [12] Ma J, Qin Z, Xie G, Qian L, Tang D. Review of mid-infrared mode-locked laser sources in the 2.0  $\mu\text{m}$ –3.5  $\mu\text{m}$  spectral region. *Appl Phys Rev* 2019;6:021367.
- [13] Wang J, Lai W, Wei K, Yang K, Zhu H, Zheng Z, et al. Generation of few-cycle pulses from a mode-locked Tm-doped fiber laser. *Opt Lett* 2021;46:2445–8.
- [14] Nelson LE, Jones DJ, Tamura K, Haus HA, Ippen EP. Ultrashort-pulse fiber ring lasers. *Appl Phys B* 1997;65:277–94.
- [15] Zhou R, Li Q, Fu HY, Nakkeeran K. Quasi-coherent noise-like pulses in a mode-locked fiber laser with a 3D rotatable polarization beam splitter. *Opt Lett* 2021;46:1305–8.
- [16] Li B, Xing J, Kwon D, Xie Y, Prakash N, Kim J, et al. Bidirectional mode-locked all-normal dispersion fiber laser. *Optica* 2020;7:961–4.
- [17] Kelly SMJ. Characteristic sideband instability of periodically amplified average soliton. *Electron Lett* 1992;28:806–7.
- [18] Zhao LM, Tang DY, Wua X, Zhang H, Lu C, Tam HY. Observation of dip-type sidebands in a soliton fiber laser. *Opt Commun* 2010;283:340–3.
- [19] Wang Y, Fu S, Zhang C, Tang X, Kong J, Lee JH, et al. Soliton distillation of pulses from a fiber laser. *J Lightwave Technol* 2021;39:2542–6.
- [20] Wang Y, Fu S, Kong J, Komarov A, Klimczak M, Buczynski R, Tang X, Tang M, Qin Y, Zhao L. Nonlinear Fourier transform enabled eigenvalue spectrum investigation for fiber laser radiation. *Photon Res* 2021;9:1531–9.
- [21] Li D, Shen D, Li L, Chen H, Tang D, Zhao L. *Appl Opt* 2015;54:7912–6.
- [22] Du Y, Shu X. Continuous-wave-induced resonant spectral sidebands in soliton fiber lasers. *Opt Lett* 2018;43:263–6.
- [23] Grudin AB, Richardson DJ, Payne DN. Passive harmonic modelocking of a fibre soliton ring laser. *Electron Lett* 1993;29:1860–1.
- [24] Grudin AB, Gray S. Passive harmonic mode locking in soliton fiber lasers. *J Opt Soc Am B* 1997;14:144–54.
- [25] Gordon JP. Dispersive perturbations of solitons of the nonlinear Schrödinger equation. *J Opt Soc Am B* 1992;9:91–7.
- [26] Liu G, Jiang X, Wang A, Chang G, Kaerner F, Zhang Z. Robust 700 MHz mode-locked Yb: fiber laser with a biased nonlinear amplifying loop mirror. *Opt Express* 2019;27:3518–27.